7-24-2015

Biofilm Formation by Borrelia Burgdorferi Sensu Lato

Venkata Arun Timmaraju
University of New Haven

Priyanka A.S. Theophilus
University of New Haven

Kunthavai Balasubramanian
University of New Haven

Shafiq Shakih
University of New Haven

David F. Luecke
University of New Haven

See next page for additional authors

Publisher Citation

Biofilm formation by Borrelia burgdorferi sensu lato. Venkata Arun Timmaraju, Priyanka A. S. Theophilus, Kunthavai Balasubramanian, Shafiq Shakih, David F. Luecke, Eva Sapi. FEMS Microbiology Letters Volume 362, Issue 15. DOI: http://dx.doi.org/10.1093/femsle/fnv120 fnv120 First published online: 24 July 2015

Comments

Authors
Venkata Arun Timmaraju, Priyanka A.S. Theophilus, Kunthavai Balasubramanian, Shafiq Shakih, David F. Luecke, and Eva Sapi

FEMS Microbiology Letters Advance Access published July 24, 2015

Biofilm formation by *Borrelia sensu lato*

Arun Timmaraju[1, 2]□, Priyanka AS Theophilus[1]□, Kunthavai Balasubramanian[1, 3], Shafiq Shakih[1], David F. Leucke[1], Eva Sapi[1]*

[1]Lyme disease research group, Department of Biology and Environmental Science, University of New Haven, West Haven, CT, USA
[2] Present address: Interpace Diagnostics, New Haven, CT, 06519
[3] Present address: Department of Hematology, Yale School of Medicine, New Haven, CT, 06520
□ Contributed equally

*** Correspondence:** Eva Sapi Ph.D., Department of Biology and Environmental Sciences, University of New Haven, 1211 Campbell Avenue, Charger Plaza LL16. West Haven, CT, 06516, USA.
esapi@newhaven.edu

Keywords: *Borrelia burgdorferi, Borrelia afzelii*, *Borrelia garinii*, biofilm, Atomic force microscopy, EPS

Abstract

Bacterial biofilms are microbial communities held together by an extracellular polymeric substance matrix predominantly composed of polysaccharides, proteins and nucleic acids. We had previously shown that *Borrelia burgdorferi sensu stricto,* the causative organism of Lyme disease in the United States is capable of forming biofilms *in vitro*. Here, we investigated biofilm formation by *Borrelia afzelii* and *Borrelia garinii*, which cause Lyme disease in Europe. Using various histochemistry and microscopy techniques, we show that *Borrelia afzelii* and *Borrelia garinii* form biofilms, which resemble biofilms formed by *Borrelia burgdorferi sensu stricto*. High-resolution atomic force microscopy revealed similarities in the ultra-structural organization of the biofilms form by three *Borrelia* species. Histochemical experiments revealed a heterogeneous organization of exopolysaccharides among the three *Borrelia* species. These results suggest that biofilm formation might be a common trait of *Borrelia* genera physiology.

1. Introduction

Lyme Borreliosis is an infectious disease caused by spirochete bacteria of the genus *Borrelia* (Burgdorfer et al., 1982). *Borrelia burgdorferi sensu stricto* genospecies which includes several *Borrelia burgdorferi* strains is the main cause of Lyme disease in the United States, whereas members of the *Borrelia sensu lato* genospecies including *Borrelia afzelii* and *Borrelia garinii* have been shown to cause the disease in Europe (Hubálek and Halouzka, 1997; Rauter and Hartung, 2005). Although the three aforementioned *Borrelia* species are the major cause of Lyme disease, their remarkably vary in clinical disease manifestation. *Borrelia burgdorferi sensu stricto* infection is associated Lyme arthritis, whereas infection with *Borrelia afzelii* is associated with Acrodermatitis chronica atrophicans (ACA, cutaneous manifestation) and infection with *Borrelia garinii* is associated with neuroborreliosis (Wang et al., 1999).

The pleomorphic *Borrelia burgdoferi* spirochete interconverts among several morphological forms including round body and cell wall deficient forms when exposed to altered environmental conditions such as high ambient pH or temperature fluctuations (Preac-Mursic et al., 1989; Brorson and Brorson, 1998; Mursic et al., 1996; Gruntar et al., 2001; Murgia and Cinco, 2004). In addition to these forms, we previously reported that *Borrelia burgdorferi* sensu stricto strains B31 and 297 are capable of forming biofilms *in vitro* (Sapi et al., 2012).

Biofilms are complex communities of free living planktonic microbes which shield constituent individuals from hostile environments (Flemming and Wingender, 2010) and are characterized by the presence of an extracellular polymeric substance (EPS). Biofilm EPS is typically composed of polysaccharides, proteins, divalent metals and extracellular DNA, which serve various functions (Flemming and Wingender, 2010; Stewart and Franklin, 2008; Sutherland, 2001; Branda et al., 2005).

The various EPS components of the *Borrelia burgdorferi sensu stricto* biofilm are sulfated mucins, non-sulfated mucins including alginate, extracellular DNA and calcium (Sapi et al., 2012). In the present study, we analyzed potential biofilm formation by *Borrelia sensu lato* species *Borrelia afzelii* and *Borrelia garinii in vitro*.

We observed that both *Borrelia afzelii* and *Borrelia garinii* are capable of biofilm formation when grown at high cell densities. The *Borrelia afzelii* and *Borrelia garinii* biofilms resemble the biofilms formed by *Borrelia burgdorferi sensu stricto* as evidenced by the presence of extracellular DNA, calcium and a tower-like organization, however, they show a heterogeneous distribution in their exopolysaccharide composition.

2. Materials and methods

Bacterial strains and culture conditions

Low passage isolates of *Borrelia burgdorferi* B31 (ATCC #35210, Burgdorfer et al., 1982), *Borrelia afzelii* BO23 (ATCC #51992, Xu et al., 1995) and *Borrelia garinii* Fuji P1 (ATCC #51383, Baranton et al., *1992*) were obtained from American Type Culture Collection. Cells were maintained in Barbour-Stoner-Kelly H (BSK-H, Sigma) media supplemented with 6% rabbit serum (Pel-Freeze) containing no antibiotics in sterile 15 ml glass tubes and incubated at 33°C with 5% CO_2. Biofilm formation was initiated by inoculating homogenous mid-log phase spirochetes (5×10^6 cells/ml) for one week in 4 well chamber glass (LAB-TEK) slides for histochemical staining experiments. Cultures were fixed with ice cold 1:1 acetone-methanol for 15 minutes at room temperature (RT) prior to histochemical staining experiments.

BacLight LIVE/DEAD staining

Cells were stained using a 1:1 mixture of LIVE/DEAD BacLight™ stain, a mixture of Syto9 and Propidium Iodide stains (LIVE/DEAD BacLight™ Bacterial Viability Kit, Invitrogen) for 15 minutes in the dark. The slides were coverslipped and images were acquired using fluorescent microscopy.

Crystal violet staining and quantitation

For crystal violet staining experiments, cells were cultured as above in 4-well chamber slides (LAB-TEK) and fixed with ice cold 1:1 acetone-methanol. Post fixation, the cells were stained with crystal

violet (0.01% in PBS, Thermo Scientific) for 10 minutes. Slides were washed with 1x phosphate buffer (PBS pH 7.4, Sigma) and imaged by bright field microscopy. For crystal violet biomass quantitation, cells were cultured for one week in a 48 well plate, pelleted and washed with 500 µl PBS by centrifugation at 1650 g for 5 minutes. The resulting pellet was resuspended in 50 µl of 0.01% crystal violet by vortexing and incubated at room temperature for 10 minutes. Crystal violet was removed by centrifugation and washing with 500 µl PBS at 1650 g for 5 minutes. The cell pellet was resuspended in 200 µl of 10% acetic acid by vortexing, followed by incubation in the dark at room temperature for 15 minutes. Post incubation, the cells were pelleted at 1650 g for 5 minutes. The supernatant was transferred to a 96-well plate and optical density was measured at 595 nm using a BioTek spectrophotometer.

MTT assay

MTT (3-(4,5-dimethylthiazol-2-yl)-2,5-diphenyltetrazolium bromide) assay was performed as previously described with brief modifications (Fallon and Hellestad, 2009). Bacteria were cultured as described above for one week in a 48 well plate and incubated with 100 µl of 2 mg/ml MTT in PBS (Sigma) for 4 hours at 33°C in dark. Post incubation, the medium was centrifuged at 1500 g for 8 minutes to pellet the biofilm and solubilized using 150 µl isopropanol for 20 minutes at RT. The precipitate was pelleted at 3000 g for 8 minutes. The supernatant was transferred to a 96 well plate and optical density was measured at 570 nm using a BioTek spectrophotometer.

Total carbohydrate assay

Total carbohydrate assay was performed as previously described with brief modifications (DuBois et al., 1956). Cells were cultured for one week in a 48 well plate, pelleted and washed with 1ml PBS by centrifugation at 1650 g for 5 minutes. To the pellet, 200 µl of sterile distilled water was added and resuspended by vortexing. Next, 100 µl of 5% phenol was added, followed by addition of 500 µl of concentrated sulfuric acid. This mixture was incubated at 33°C for 20 minutes and optical density was measured at 485 nm using a BioTek spectrophotometer.

Statistical analysis

Statistical analyses were performed using GraphPad Prism version 6.00 for Windows (GraphPad Software, La Jolla California USA, www.graphpad.com). Quantitative data are presented as mean ± S.E. of three independent experiments, performed in triplicates. Differences between groups were considered statistically significant at $p<0.05$, compared using unpaired Student's t-test.

Atomic force microscopy

Biofilm rich stationary cultures were centrifuged at 6000×g for 5 minutes at room temperature and the resultant cell pellets were gently resuspended in PBS and spotted onto Superfrost™ Plus slides (Fisher). Contact mode AFM imaging in air was performed on a Nanosurf Easyscan 2 AFM (Nanosurf) using qp-SCONT probes (Nanosensors Inc). Images were processed using Gwyddion software (Nečas and Klapetek, 2012).

Spicer and Meyer staining

Spicer and Meyer sequential staining was performed as previously described (Spicer and Meyer, 1960; Sapi et al., 2012). First, fixed slides were stained aldehyde fuchsine solution (0.5% fuchsine dye dissolved in 6% acetaldehyde in 70% ethanol with 1% concentrated hydrochloric acid) for 20 minutes, and dipped in 70% ethanol for 1 min and double distilled water for 1 minute. Next, slides were stained with 1% Alcian blue in 3% acetic acid, pH 2.5 for 30 minutes, rinsed in double distilled

water for 3 minutes and passed through a chilled graded ethanol series (50%, 70% and 95% ethanol for 3 minutes each) and dipped in chilled xylene for 2 minutes followed by mounting in Permount (Fisher Scientific). Fuchsine and Alcian blue 8GX dyes were purchased from Sigma-Aldrich.

Alginate immunofluorescence

Immunofluorescent detection of alginate was performed as previously described (Sapi et al., 2012). Briefly, fixed cells were blocked with 10% normal goat serum (Thermo Scientific) in PBS/0.5% bovine serum albumin (BSA, Sigma) for 30 minutes at RT. Slides were then incubated with anti-alginate rabbit polyclonal IgG antibody (1:100 dilution in dilution buffer - PBS pH 7.4+0.5% BSA) overnight in a humidified chamber, followed by incubation with DyLight 594 conjugated goat anti-rabbit IgG secondary antibody (1:200, Thermo Scientific) for 1 hour in at RT. Slides were then incubated with FITC tagged *Borrelia* rabbit polyclonal IgG antibody (1:50, Thermo Scientific # PA1-73005) for 1 hour at RT. Slides were then counterstained with 4',6-diamidino-2-phenylindole (DAPI, Sigma, diluted 1:1000 in PBS) and mounted with Permaflour (Fisher).

Lectin binding analysis

Fixed cells were washed with 0.1% BSA in PBS pH 7.4 and incubated with 20 ng/ml FITC conjugated HHA and MOA lectins (EY Laboratories) for 2 hrs at RT in dark. Post incubation, slides were washed with 0.1% BSA in PBS pH 7.4, counterstained with DAPI and mounted with Permaflour.

Calcium staining

Fixed cells were stained with 2% Alizarin Red-S (pH 4.2, Sigma) for four minutes at RT. Following incubation, slides were washed twice using double distilled water, dehydrated through graded alcohols and mounted using Permount (Fisher Scientific).

Extracellular DNA staining

Extracellular DNA was stained with 1 mM DDAO [7-hydroxy-9H-(1, 3-dichloro-9, 9 dimethylacridin-2-one)] for 30 min at 37° C in dark. DDAO-treated slides were then washed two times using TE buffer, counterstained with DAPI and mounted using Permaflour.

Image acquisition and processing

Images from histochemical staining experiments were acquired on a Leica DM2500 microscope with a DFC500 camera. For fluorescent staining merged micrographs, raw images were sharpened to remove lens blur using Photoshop CS6 (Adobe) and images from different channels were stacked using ImageJ (NIH) and are displayed as maximum intensity z-projections.

3. Results

Borrelia burgdorferi, *Borrelia afzelii* and *Borrelia garinii* form biofilms *in vitro*

We hypothesized that *Borrelia afzelii* and *Borrelia garinii* form biofilms when grown at a high cell density, similar to the biofilms formed by *Borrelia burgdorferi* sensu stricto strains. To address this question, we seeded mid log phase $5x10^6$ *Borrelia afzelii* and *Borrelia garinii* cells and grew them for one week under standard *Borrelia burgdorferi* B31 culture conditions of 33°C and 5% CO_2 in BSK-H medium containing 6% rabbit serum (Sapi et al., 2012).

At the end of one week, cultures were observed by BacLight LIVE/DEAD staining and crystal violet staining. Fluorescence micrographs of BacLight staining showed predominantly live cells, with some dead cells in the aggregates formed by *Borrelia burgdorferi* B31, *Borrelia afzelii* and *Borrelia garinii* (Figure 1 A-C). Bright field micrographs of crystal violet stained cultures show that *Borrelia afzelii* and *Borrelia garinii* form biofilm like aggregates, surrounded by planktonic spirochetes similar to the biofilms formed by *Borrelia burgdorferi* (Figure 1 D-F).

To quantitatively assess biofilm development, we performed the MTT and crystal violet assays to analyze differences in growth kinetics and biomass of the aggregates formed by the three *Borrelia* species. For these assays, $5x10^6$ cells were grown in 48 well plates for one week and the total contents of the well i.e. attached and floating biofilms, were harvested for analysis.

MTT assay revealed that *Borrelia garinii* has significantly low growth kinetics ($n=3$, $p\leq0.05$) compared to *Borrelia afzelii* and *Borrelia burgdorferi* B31, which do not differ in their growth rates ($n=3$, $p\geq0.05$) (Figure 1G). Crystal violet assay showed that the biomass between the three *Borrelia* species did not differ significantly ($n=3$, $p\geq0.05$) (Figure 1H).

Ultra structural features of the *Borrelia* biofilms

We and others have previously used atomic force microscopy (AFM) to study the internal organization of bacterial biofilms (Oh et al., 2009; Cross et al., 2006; Sapi et al., 2012; Oh et al., 2007). Here, we used contact mode AFM to get a closer look at the morphology and topography of *Borrelia* aggregates.

Morphologically, compared to *Borrelia burgdorferi* B31 biofilms (Figure 2A), *Borrelia afzelii* aggregates are composed of enmeshed spirochetes (Figure 2B, 3A), whereas *Borrelia garinii* aggregates have a relatively higher proportion of round-bodies (Figure 2C, 3B). Furthermore, aggregates formed by the three *Borrelia* species are organized as "towers", with pits and protrusions (Figure 2D-F, 3C) (Hall-Stoodley et al., 2008; Fey and Olson, 2010; Sapi et al., 2012)

Topographically, the tower organization of *Borrelia afzelii* and *Borrelia garinii* biofilm like aggregates may be due to the presence of an extracellular polymeric substance (EPS) as observed in the case of *Borrelia burgdorferi*. We estimated the EPS by measuring the heights of biofilm aggregates by extracting the profiles of the scans from the AFM phase images and observed that the EPS heights of *Borrelia* biofilm like aggregates of all three species are typically ~1 μM tall. A representative x-y surface plot shows the typical height profile and the presence of pits (Fig 3C) and protrusions across aggregates formed by the three *Borrelia* species (Figure 2D-F).

Are *Borrelia* aggregates true biofilms?

All three *Borrelia* species grow as aggregates (Figure 1) and assemble an EPS as indicated by the AFM peaks (Figure 2). To establish whether these aggregates are indeed biofilms, we studied the various EPS components typically found in bacterial biofilms including mucins, carbohydrates, calcium and extracellular DNA using various histochemical staining techniques.

Mucopolysaccharide rich matrix of *Borrelia* biofilms

To assess the presence of polysaccharides/ sugars in the biofilm EPS; we used Spicer & Meyer Fuchsine-Alcian blue sequential histological staining method. This method has been extensively used to study the mucin rich gastrointestinal tissues (Spicer and Meyer, 1960). Here, we use Spicer & Meyer staining to differentiate between sulfated and non-sulfated/carboxylated. Representative dark field micrographs show that *Borrelia burgdorferi* B31 aggregates are rich in non-sulfated/carboxylated mucins (blue staining) in the center of the aggregates and are surrounded possibly by sulfomucins and proteoglycans (fuchsia/ purple staining) (Figure 3A-B). *Borrelia afzelii* (Figure 3C-D) and *Borrelia garinii* (Figure 3E-F) are rich in non-sulfated/carboxylated mucins in the center of the aggregates but do not appear to be enriched for sulfomucins at the edges. Interestingly, there is significant inter-species and intra-species heterogeneity in Spicer & Meyer staining patterns, which did not correlate with biofilm sizes and adherence.

To assess whether there were any differences in the total carbohydrate secreted, we measured carbohydrate content using the total carbohydrate assay. We observed that *Borrelia afzelii* contained significantly more amounts of carbohydrates than *Borrelia burgdorferi* B31 ($n=3$, $p \leq 0.05$). *Borrelia burgdorferi* and *Borrelia garinii,* and *Borrelia afzelii* and *Borrelia garinii* did not differ significantly in carbohydrate content ($n=3$, $p \geq 0.05$) (Figure 3G).

Next, we looked at whether alginate, a non-sulfated mucopolysaccharide present in *Borrelia burgdorferi sensu stricto* biofilms (Sapi et al., 2012), is present in *Borrelia afzelii* and *Borrelia garinii* biofilm like aggregates. Immunofluorescent staining using the anti-alginate antibody showed the presence of alginate in *Borrelia afzelii* and *Borrelia garinii* aggregates (Figure 4). This is consistent with Spicer and Meyer staining indicating the presence of non-sulfated mucopolysaccharides.

These experiments suggest that *Borrelia afzelii* and *Borrelia garinii* also form mucoid biofilms but differ in the organization of the various mucins. We reasoned that the differences in Spicer and Meyer staining may be due to the presence of other EPS polysaccharides.

Pseudomonas aeruginosa strains have three major EPS polysaccharides, namely Pel, Psl and alginate with Pel and Psl playing important roles in biofilm attachment and development whereas alginate is expressed only by mucoid strains (Ma et al., 2007). To address whether the differences in the EPS organization may be due to Psl polysaccharides, we used lectin-binding analyses.

Lectins are glycoproteins of animal, plant or microbial origin, which specifically bind carbohydrates and have been used to identify various biofilm EPS components. Lectin HHA (from *Hippeastrum hybrid*) and lectin MOA (from *Marasmium oreades*) have been used extensively to study the presence of Psl exopolysaccharides in *Pseudomonas aeruginosa*. HHA lectin binds mannosyl units in polysaccharides whereas MOA is a mushroom lectin which binds galactosyl residues on the ends of glycan chains (Ma et al., 2007; Hall-Stoodley et al., 2008).

Borrelia burgdorferi, *Borrelia afzelii* and *Borrelia garinii* were stained with FITC conjugated HHA and MOA lectins. Merged fluorescent micrographs of lectin staining (green) and DNA staining (blue). In *Borrelia burgdorferi* B31 aggregates, HHA lectin staining was observed throughout the biofilm, whereas in *Borrelia afzelii* and *Borrelia garinii*, HHA lectin staining was observed internal of the biofilm (Figure 5 A-F). MOA lectin staining was observed throughout *Borrelia burgdorferi* B31 and *Borrelia afzelii* aggregates, whereas in *Borrelia garinii* aggregates, MOA lectin staining was observed at the periphery (Figure 5 G-L). These results indicate the presence of a Psl-like EPS, which may interfere with the sulfomucin organization, leading to differences in Spicer-Meyer staining patterns (Spicer and Meyer, 1960; Sapi et al., 2012).

Presence of calcium in *Borrelia* biofilms

Previously, we identified the presence of calcium in biofilms formed by *Borrelia burgdorferi sensu stricto* strains (Sapi et al., 2012). To examine whether *Borrelia afzelii* and *Borrelia garinii* aggregates also contain calcium, we used a calcium specific stain, Alizarin Red S. Merged dark field and fluorescence micrographs revealed the presence of calcium in the aggregates formed by *Borrelia afzelii* and *Borrelia garinii* but not on the surrounding spirochetes (Figure 6).

Presence of extracellular DNA in *Borrelia* biofilms

Another component of the EPS is extracellular DNA, which plays an important role in substrate attachment and stabilization of biofilm. Using an eDNA specific stain DDAO, we show that the aggregates formed by *Borrelia burgdorferi, Borrelia afzelii* and *Borrelia garinii* contain significant amounts of eDNA, internal to the biofilm which is not found associated with isolated spirochetes, however there are no differences in staining patterns among the three species (Figure 7 A-F).

Discussion

In this paper, we provide evidence that *Borrelia afzelii* and *Borrelia garinii* of the *Borrelia sensu lato* genospecies can form biofilms *in vitro*. These biofilms are viable and are either surface adherent or floating and show considerable heterogeneity in size and shapes, as observed for various biofilm forming bacteria (Stewart and Franklin, 2008). Using atomic force microscopy coupled with histochemical staining techniques, we identify similarities and differences in the biofilms formed by the three species.

Quantitative experiments showed that *Borrelia burgdorferi* and *Borrelia afzelii* grow at a similar rate, whereas the growth of *Borrelia garinii* is significantly slower. Despite the differences in growth rates, the total biofilm biomass of the three species did not differ. Interestingly all three species differ in their total carbohydrate content which suggest that they might produce different amounts of extracellular polysaccharides.

Previously, we used atomic force microscopy (AFM) to characterize various stages in biofilm formation by *Borrelia burgdorferi sensu stricto* (Sapi et al., 2012). Here, we used AFM to identify

potential morphological differences in the biofilm structures of different *Borrelia* species. Consistent with our previous data, *Borrelia burgdorferi sensu stricto* forms a matrix-dense biofilm (Sapi et al., 2012), whereas *Borrelia afzelii* forms a network-like biofilm and *Borrelia garinii* biofilm has a relatively higher proportion of round-bodies.

Topographical analysis did not show any significant differences in the heights of different *Borrelia* biofilms. These differences may not be characteristic of the biofilms formed these species, but may be attributed to the differences in the diameters of the biofilm i.e. taller biofilm heights may correspond to wider biofilm diameters irrespective of the bacteria being studied. Another topographical feature of *Borrelia* biofilms is the presence of pits and protrusions, as observed in the spirochete *Leptospira*, which forms biofilms by cell-cell aggregation (Triampo et al., 2004; Ristow et al., 2008). Recently, it was reported that an unrelated bacterium, *Chromobacterium violaceum* forms biofilms containing invaginations and extrusions that resemble the pits and protrusions of Borrelia biofilms (Kamaeva et al., 2014).

The core of the EPS of the three *Borrelia* biofilms is rich in the non-sulfated/ carboxylated mucin - alginate, indicating the presence of a mucoid biofilm. Alginate is a negatively charged polymer which in the presence of divalent cations forms a gelatinous mucoid matrix (Remminghorst and Rehm, 2006). In *Azotobacter* biofilms, alginate plays a protective role by maintaining capsule structural integrity during unfavorable conditions (Clementi, 1997). In some strains of *Pseudomonas aeruginosa*, the causative organism of cystic fibrosis, alginate is a major component of the mucoid biofilm, which confers resistance to oxidative stress and host immune surveillance (Hentzer et al., 2001).

We observed differences in the organization of sulfomucins around the biofilm edges of the three *Borrelia* species. We reasoned that the differences might be due to the presence of a Psl-like polysaccharide. Using lectin staining we identified that Borrelia biofilms are rich in mannose and galactose and hence possess a Psl like polysaccharide as found in *P. aeruginosa* biofilms. (Ma et al., 2007). However, the staining patterns of MOA and HHA lectins of Borrelia biofilms do not account for the differences in sulfomucin staining.

The three *Borrelia* species studied here possess an EPS that contains Psl-like polysaccharide as well as alginate, and *Borrelia* biofilms retain both Psl and alginate at maturation, unlike the mucoid *P. aeruginosa* strains, which switch from Psl to alginate. Psl deletion mutants in mucoid *P. aeruginosa* mucoid strains show deficiency in biofilm formation suggesting that the Psl polysaccharides are required for biofilm formation and alginate expression is observed after stable biofilm adhesion (Ma et al., 2006; Schurr, 2013). We suspect that a Psl-like polysaccharides secretion precedes alginate secretion during *Borrelia* biofilm development.

Although the Borrelia biofilms show differences in polysaccharide organization and morphology, they are similar in the organization of calcium and extracellular DNA. Calcium, plays a dual role by stabilizing the alginate matrix and chelating eDNA, which increases biofilm matrix stability (Sapi et al., 2012). Extracellular DNA is present internal to the Borrelia biofilm, consistent with its role in

facilitating biofilm formation (Whitchurch et al., 2002), intercellular adhesion (Vilain et al., 2009) and substrate attachment (Gloag et al., 2013). Furthermore, under altered physiological conditions, eDNA contributes to antimicrobial activity by chelating cations with its inherent negative charge (Mulcahy et al., 2008).

In summary, results obtained from this study indicate that the aggregates formed by *Borrelia afzelii* and *Borrelia garinii* are biofilms that resemble the biofilms formed by *Borrelia burgdorferi sensu stricto*. Taken together, we suggest that biofilm formation is a common trait for Borrelia genera, which could confer survival advantages during unfavorable conditions.

4. Acknowledgements

The study was supported by University of New Haven and grants from the Lymedisease.org**,** Tom Crawford's Leadership Children's Foundation, Midwest Lyme Foundation, National Philanthropic Trust and Warman Family to ES and an anonymous donor-advised fund of the NH Charitable Foundation to PAST. Microscopes used in this study were donated to the University of New Haven Lyme Disease Research Group by Lymedisease.org, Schwartz foundation, Lyme Research Alliance and Lyme Disease Association. The authors thank Dr. Gerald B. Pier, Harvard University for kindly donating the anti-alginate antibody. A part of this project involves work towards KB and SS's master's thesis.

5. Author contributions

AT, PAST, KB, SS and DFL performed the experiments. AT and ES designed the study, interpreted the data and wrote the manuscript.

6. References

Baranton, G., Postic, D., Saint Girons, I., Boerlin, P., Piffaretti, J. C., Assous, M., & Grimont, P. A. (1992). Delineation of Borrelia burgdorferi sensu stricto, Borrelia garinii sp. nov., and group VS461 associated with Lyme borreliosis. *Int. J. Syst. Bacteriol*. 42: 378-383, 1992.

Branda, S. S., Vik, S., Friedman, L., and Kolter, R. (2005). Biofilms: the matrix revisited. *Trends Microbiol.* 13, 20–6. doi:10.1016/j.tim.2004.11.006.

Brorson, O., and Brorson, S. H. (1998). In vitro conversion of Borrelia burgdorferi to cystic forms in spinal fluid, and transformation to mobile spirochetes by incubation in BSK-H medium. *Infection* 26, 144–50.

Burgdorfer, W., Barbour, A., Hayes, S., Benach, J., Grunwaldt, E., and Davis, J. (1982). Lyme disease-a tick-borne spirochetosis? *Science (80-.).* 216, 1317–1319. doi:10.1126/science.7043737.

Clementi, F. (1997). Alginate production by Azotobacter vinelandii. *Crit. Rev. Biotechnol.* 17, 327–61. doi:10.3109/07388559709146618.

Cross, S. E., Kreth, J., Zhu, L., Qi, F., Pelling, A. E., Shi, W., and Gimzewski, J. K. (2006). Atomic force microscopy study of the structure-function relationships of the biofilm-forming bacterium Streptococcus mutans. *Nanotechnology* 17, S1–7. doi:10.1088/0957-4484/17/4/001.

DuBois, M., Gilles, K. a., Hamilton, J. K., Rebers, P. a., and Smith, F. (1956). Colorimetric Method for Determination of Sugars and Related Substances. *Anal. Chem.* 28, 350–356. doi:10.1021/ac60111a017.

Fallon, A. M., and Hellestad, V. J. (2009). Standardization of a colorimetric method to quantify growth and metabolic activity of Wolbachia-infected mosquito cells. *In Vitro Cell. Dev. Biol. Anim.* 44, 351–6. doi:10.1007/s11626-008-9129-6.

Flemming, H.-C., and Wingender, J. (2010). The biofilm matrix. *Nat. Rev. Microbiol.* 8, 623–33. doi:10.1038/nrmicro2415.

Fey, P.D., and Olson M.E. (2010). Current concepts in biofilm formation of Staphylococcus epidermidis. *Future microbiol,* 5:6: 917-933. doi:10.2217/fmb.10.56.

Gloag, E. S., Turnbull, L., Huang, A., Vallotton, P., Wang, H., Nolan, L. M., Mililli, L., Hunt, C., Lu, J., Osvath, S. R., et al. (2013). Self-organization of bacterial biofilms is facilitated by extracellular DNA. *Proc. Natl. Acad. Sci. U. S. A.* 110, 11541–6. doi:10.1073/pnas.1218898110.

Gruntar, I., Malovrh, T., Murgia, R., and Cinco, M. (2001). Conversion of Borrelia garinii cystic forms to motile spirochetes in vivo. *APMIS* 109, 383–8.

Hall-Stoodley, L., Nistico, L., Sambanthamoorthy, K., Dice, B., Nguyen, D., Mershon, W. J., Johnson, C., Hu, F. Z., Stoodley, P., Ehrlich, G. D., et al. (2008). Characterization of biofilm matrix, degradation by DNase treatment and evidence of capsule downregulation in Streptococcus pneumoniae clinical isolates. *BMC Microbiol.* 8, 173. doi:10.1186/1471-2180-8-173.

Hentzer, M., Teitzel, G. M., Balzer, G. J., Heydorn, A., Molin, S., Givskov, M., and Parsek, M. R. (2001). Alginate Overproduction Affects Pseudomonas aeruginosa Biofilm Structure and Function. *J. Bacteriol.* 183, 5395–5401. doi:10.1128/JB.183.18.5395-5401.2001.

Hubálek, Z., and Halouzka, J. (1997). Distribution of Borrelia burgdorferi sensu lato genomic groups in Europe, a review. *Eur. J. Epidemiol.* 13, 951–7.

Kamaeva, A. a, Vasilchenko, A. S., and Deryabin, D. G. (2014). Atomic Force Microscopy Reveals a Morphological Differentiation of Chromobacterium violaceum Cells Associated with Biofilm Development and Directed by N-Hexanoyl-L-Homoserine Lactone. *PLoS One* 9, e103741. doi:10.1371/journal.pone.0103741.

Ma, L., Jackson, K. D., Landry, R. M., Parsek, M. R., and Wozniak, D. J. (2006). Analysis of Pseudomonas aeruginosa conditional psl variants reveals roles for the psl polysaccharide in adhesion and maintaining biofilm structure postattachment. *J. Bacteriol.* 188, 8213–21. doi:10.1128/JB.01202-06.

Ma, L., Lu, H., Sprinkle, A., Parsek, M. R., and Wozniak, D. J. (2007). Pseudomonas aeruginosa Psl is a galactose- and mannose-rich exopolysaccharide. *J. Bacteriol.* 189, 8353–6. doi:10.1128/JB.00620-07.

Mulcahy, H., Charron-Mazenod, L., and Lewenza, S. (2008). Extracellular DNA chelates cations and induces antibiotic resistance in Pseudomonas aeruginosa biofilms. *PLoS Pathog.* 4, e1000213. doi:10.1371/journal.ppat.1000213.

Murgia, R., and Cinco, M. (2004). Induction of cystic forms by different stress conditions in Borrelia burgdorferi. *APMIS* 112, 57–62.

Mursic, V. P., Wanner, G., Reinhardt, S., Wilske, B., Busch, U., and Marget, W. (1996). Formation and cultivation of Borrelia burgdorferi spheroplast-L-form variants. *Infection* 24, 218–26.

Nečas, D., and Klapetek, P. (2012). Gwyddion: an open-source software for SPM data analysis. *Cent. Eur. J. Phys.* 10, 181–188. doi:10.2478/s11534-011-0096-2.

Oh, Y. J., Jo, W., Yang, Y., and Park, S. (2007). Influence of culture conditions on Escherichia coli O157:H7 biofilm formation by atomic force microscopy. *Ultramicroscopy* 107, 869–74. doi:10.1016/j.ultramic.2007.01.021.

Oh, Y. J., Lee, N. R., Jo, W., Jung, W. K., and Lim, J. S. (2009). Effects of substrates on biofilm formation observed by atomic force microscopy. *Ultramicroscopy* 109, 874–80. doi:10.1016/j.ultramic.2009.03.042.

Preac-Mursic, V., Weber, K., Pfister, H. W., Wilske, B., Gross, B., Baumann, a, and Prokop, J. (1989). Survival of Borrelia burgdorferi in antibiotically treated patients with Lyme borreliosis. *Infection* 17, 355–9.

Rauter, C., and Hartung, T. (2005). Prevalence of Borrelia burgdorferi Sensu Lato Genospecies in Ixodes ricinus Ticks in Europe□: a Metaanalysis Prevalence of Borrelia burgdorferi Sensu Lato Genospecies in Ixodes ricinus Ticks in Europe□: a Metaanalysis. 71. doi:10.1128/AEM.71.11.7203.

Remminghorst, U., and Rehm, B. H. a (2006). Bacterial alginates: from biosynthesis to applications. *Biotechnol. Lett.* 28, 1701–12. doi:10.1007/s10529-006-9156-x.

Ristow, P., Bourhy, P., Kerneis, S., Schmitt, C., Prevost, M.-C., Lilenbaum, W., and Picardeau, M. (2008). Biofilm formation by saprophytic and pathogenic leptospires. *Microbiology* 154, 1309–17. doi:10.1099/mic.0.2007/014746-0.

Sapi, E., Bastian, S. L., Mpoy, C. M., Scott, S., Rattelle, A., Pabbati, N., Poruri, A., Burugu, D., Theophilus, P. a S., Pham, T. V, et al. (2012). Characterization of biofilm formation by Borrelia burgdorferi in vitro. *PLoS One* 7, e48277. doi:10.1371/journal.pone.0048277.

Schurr, M. J. (2013). Which bacterial biofilm exopolysaccharide is preferred, Psl or alginate? *J. Bacteriol.* 195, 1623–6. doi:10.1128/JB.00173-13.

Spicer, S. S., and Meyer, D. B. (1960). Histochemical differentiation of acid mucopolysaccharides by means of combined aldehyde fuchsin-alcian blue staining. *Tech. Bull. Regist. Med. Technol.* 30, 53–60.

Stewart, P. S., and Franklin, M. J. (2008). Physiological heterogeneity in biofilms. *Nat. Rev. Microbiol.* 6, 199–210. doi:10.1038/nrmicro1838.

Sutherland, I. (2001). Biofilm exopolysaccharides: a strong and sticky framework. *Microbiology* 147, 3–9.

Triampo, W., Doungchawee, G., Triampo, D., Wong-Ekkabut, J., and Tang, I.-M. (2004). Effects of static magnetic field on growth of leptospire, Leptospira interrogans serovar canicola: immunoreactivity and cell division. *J. Biosci. Bioeng.* 98, 182–6. doi:10.1016/S1389-1723(04)00263-4.

Vilain, S., Pretorius, J. M., Theron, J., and Brözel, V. S. (2009). DNA as an adhesin: Bacillus cereus requires extracellular DNA to form biofilms. *Appl. Environ. Microbiol.* 75, 2861–8. doi:10.1128/AEM.01317-08.

Wang, G., Van Dam, A. P., Schwartz, I., & Dankert, J. (1999). Molecular typing of Borrelia burgdorferisensu lato: taxonomic, epidemiological, and clinical implications. *Clin microbiol rev*, *12*(4), 633-653.

Whitchurch, C. B., Tolker-Nielsen, T., Ragas, P. C., and Mattick, J. S. (2002). Extracellular DNA required for bacterial biofilm formation. *Science* 295, 1487. doi:10.1126/science.295.5559.1487.

Xu, Y., & Johnson, R. C. (1995). Analysis and comparison of plasmid profiles of Borrelia burgdorferi sensu lato strains. *J. Clin. Microbiol*, 33: 2679-2685.

Figure legends

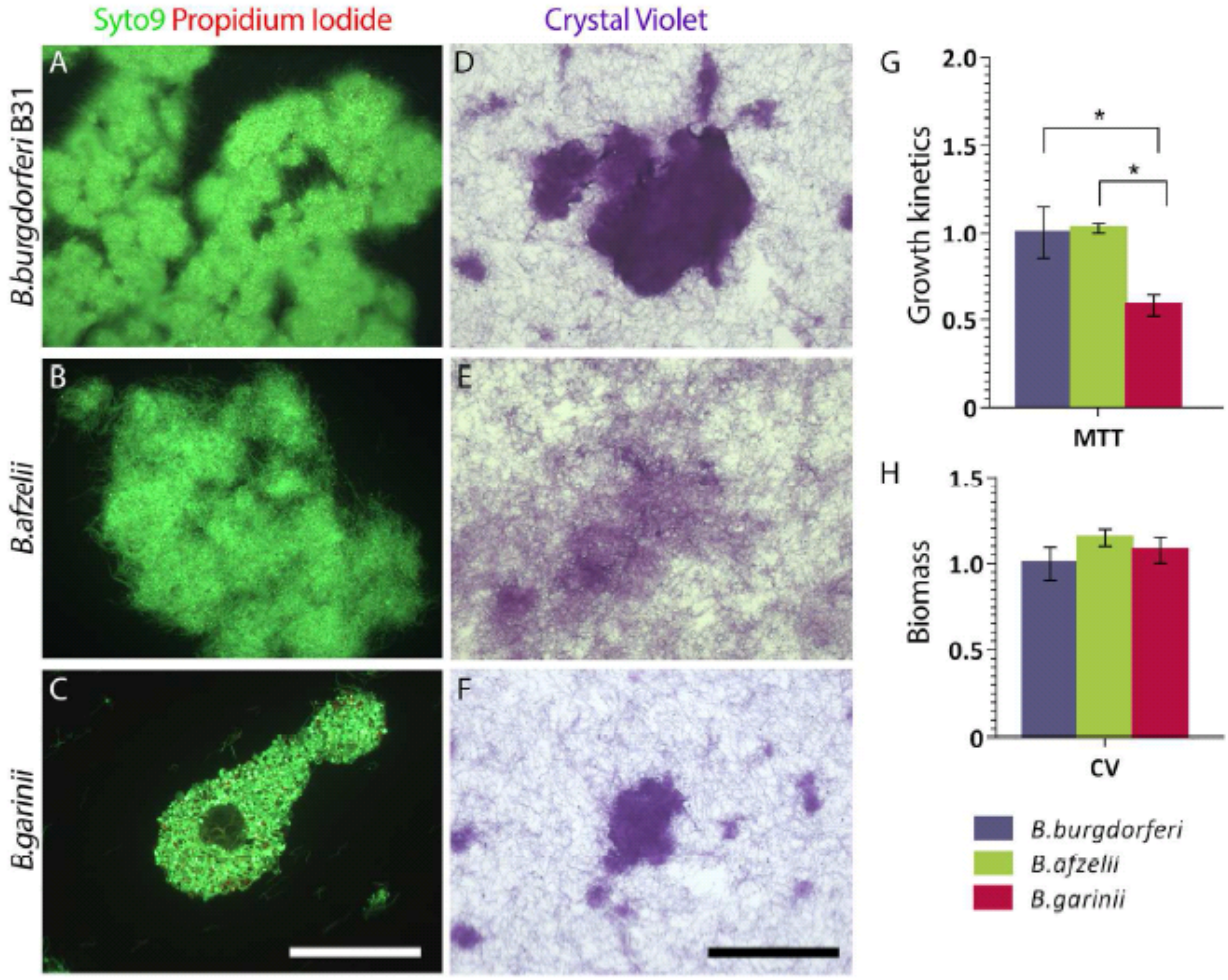

Fig 1. Biofilm like aggregate formation by *Borrelia* species. Panels A-C show fluorescent micrographs of LIVE/DEAD staining of floating Borrelia aggregates; Scale bar – 100 µm and D-F show brightfield micrographs of crystal violet staining of attached *Borrelia* aggregates, surrounded by spirochetes; Scale bar – 200 µm, of $5x10^6$ cells of *Borrelia burgdorferi* B31 (A, D) *Borrelia afzelii* and (B, E) and *Borrelia garinii* (C, F) cultures grown for 1 week, respectively. Panels G-H show that the three *Borrelia* species grow at different rates (MTT assay), but do not differ in total biomass (Crystal violet assay) (n=3, *P≤0.05).

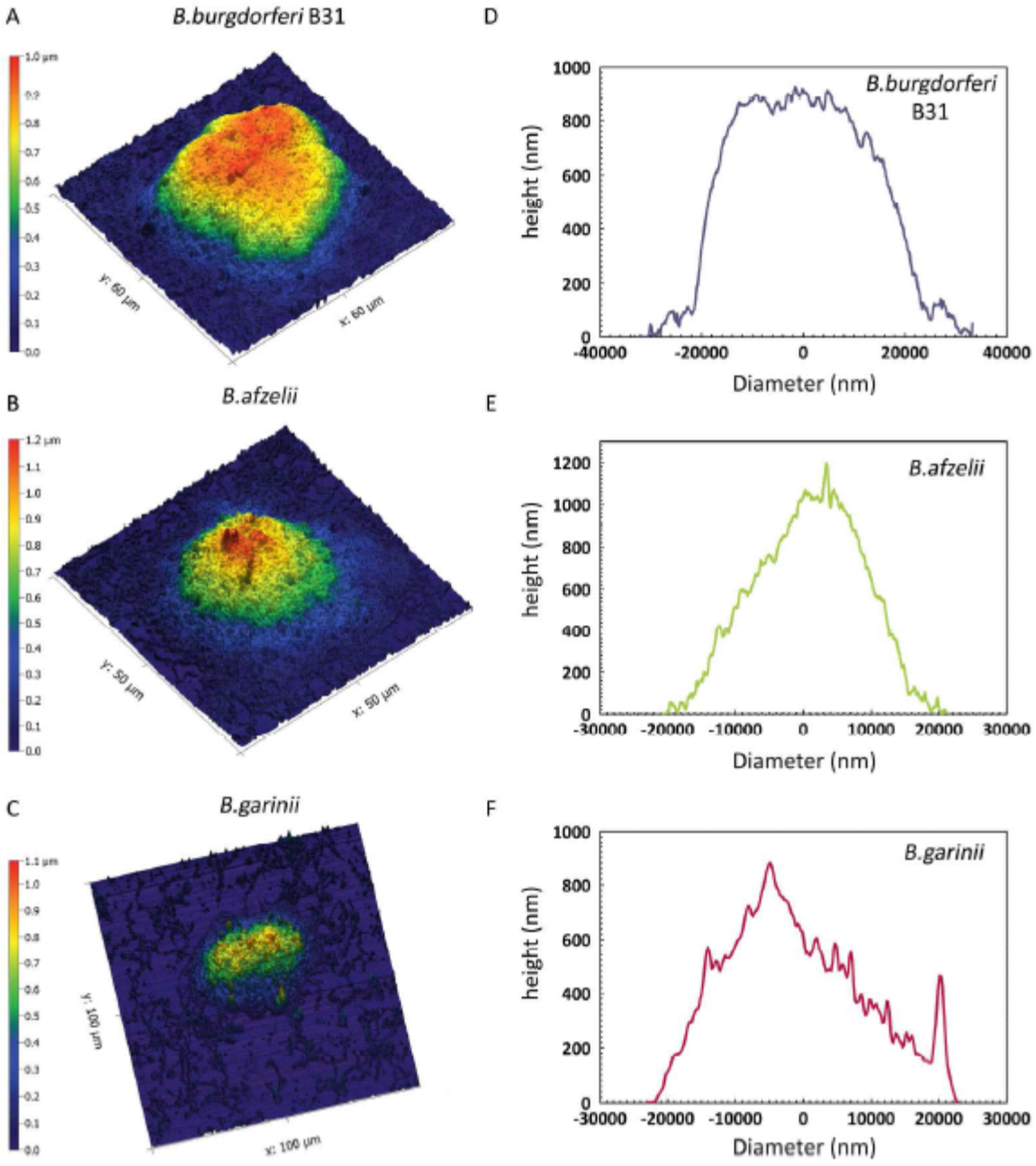

Fig 2. Ultrastructure of biofilm like aggregates formed by *Borrelia* species. Representative atomic force microscopy scans and profile graphs show ultrastructure and topology of (A, B) *Borrelia burgdorferi* B31 (C, D) *Borrelia afzelii* and (E, F) *Borrelia garinii* aggregates. AFM images shown here are pseudo-colored using Gwyddion software and the color gradient is a measure of height in µm. Graphs show x-y scatter plots of dry height corresponding-diameter measurements from AFM phase image profiles.

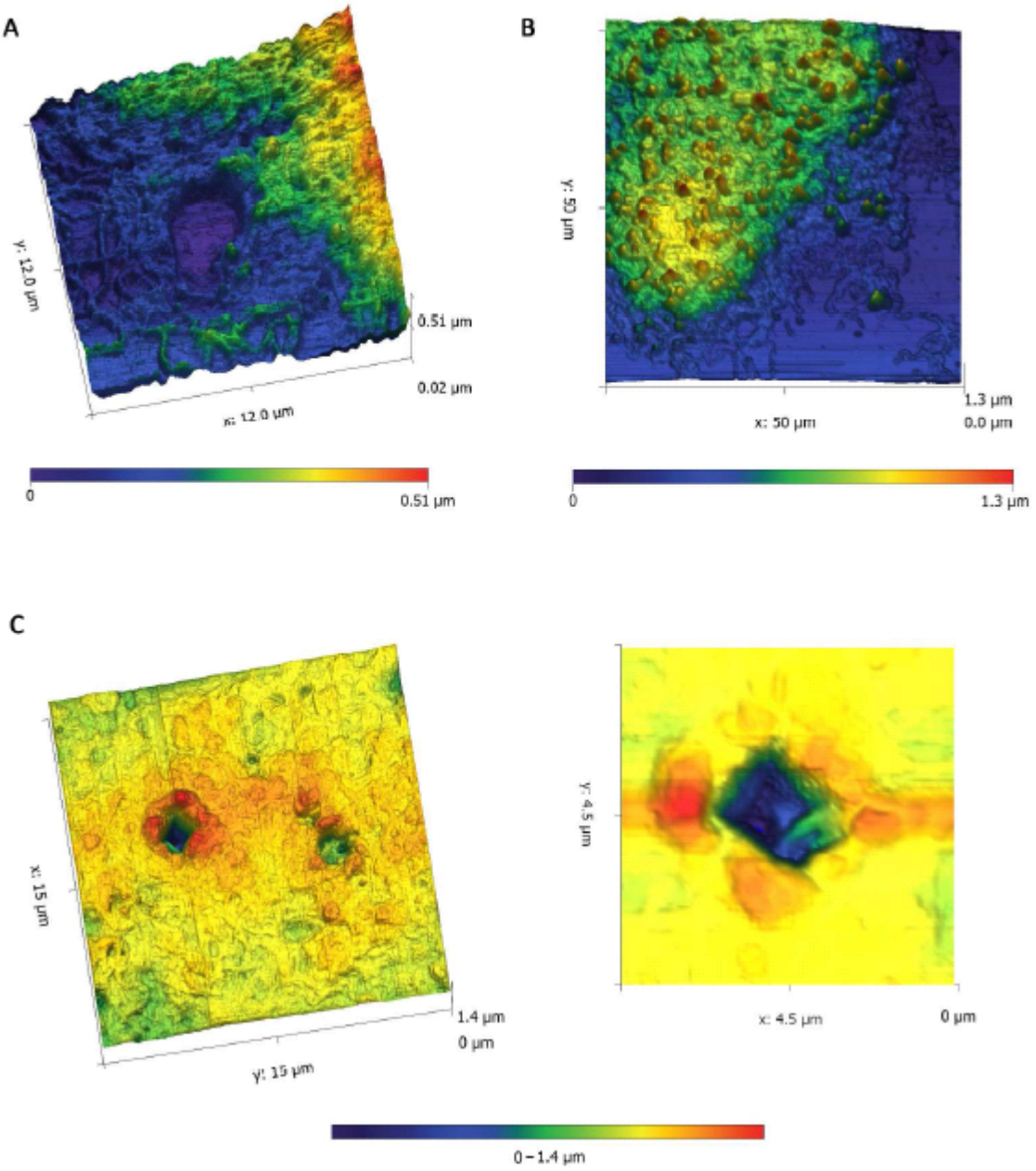

Fig 3. A-B) Atomic force micrographs of biofilm edges of *Borrelia afzelii* and *Borrelia garinii* show reticular networks and round-body enriched morphologies of the biofilms respectively. C) Higher resolution scans *Borrelia afzelii* biofilm showing a pit (invagination) deeper than µm. AFM images shown here are pseudo-colored using Gwyddion software and the color gradient is a measure of height in µm.

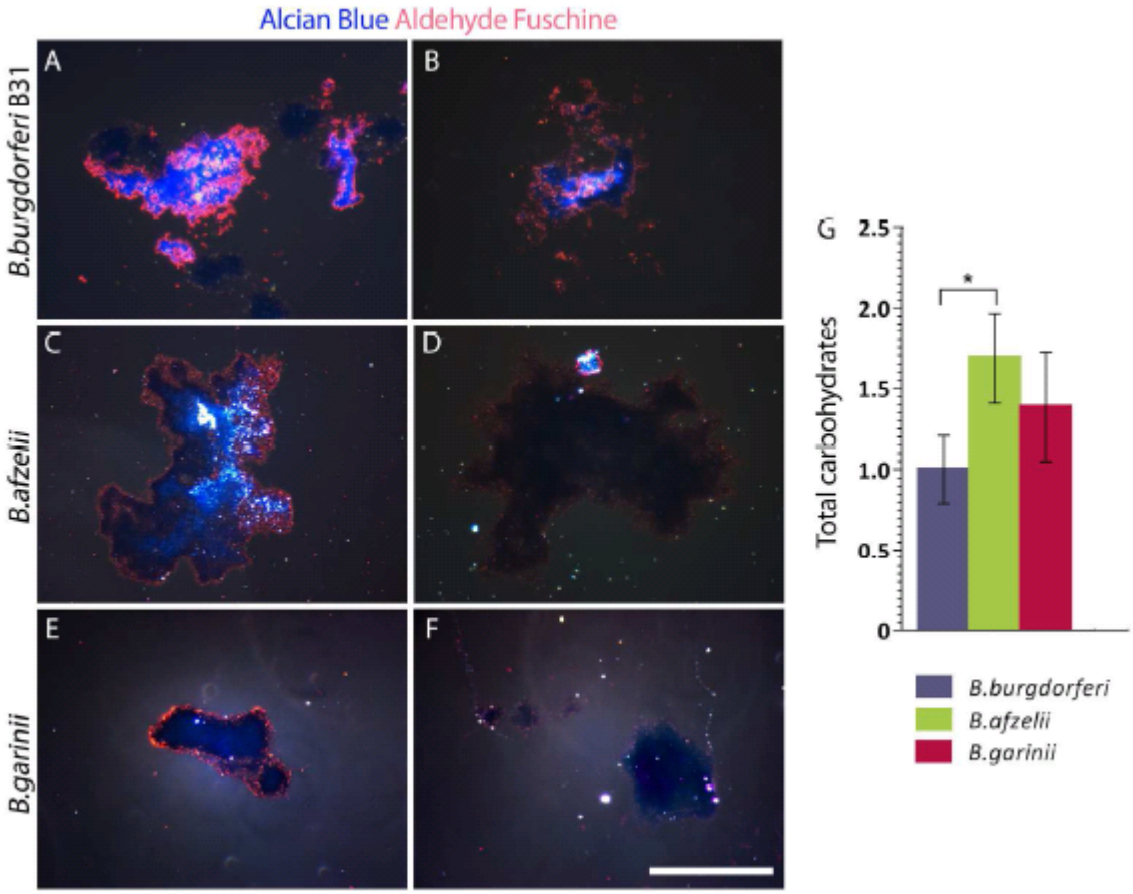

Fig 4. Mucoid phenotype of *Borrelia* aggregates. Representative dark field micrographs of sequential Spicer & Meyer staining show differences and heterogeneity in the mucin composition among aggregates formed by (A-B) *Borrelia burgdorferi* B31 (C-D) *Borrelia afzelii* and (E-F) *Borrelia garinii.* Scale bar - 100 µm. Color index: Red/Fuchsia - weakly acidic sulfomucins; purple - strongly acidic sulfomucins and/or sulfated proteoglycans; blue - non-sulfated, carboxylated mucins. (G) *Borrelia* species grown for 1 week at high confluence differ in their total carbohydrate content as measured by total carbohydrate assay (n=3, * P≤0.05).

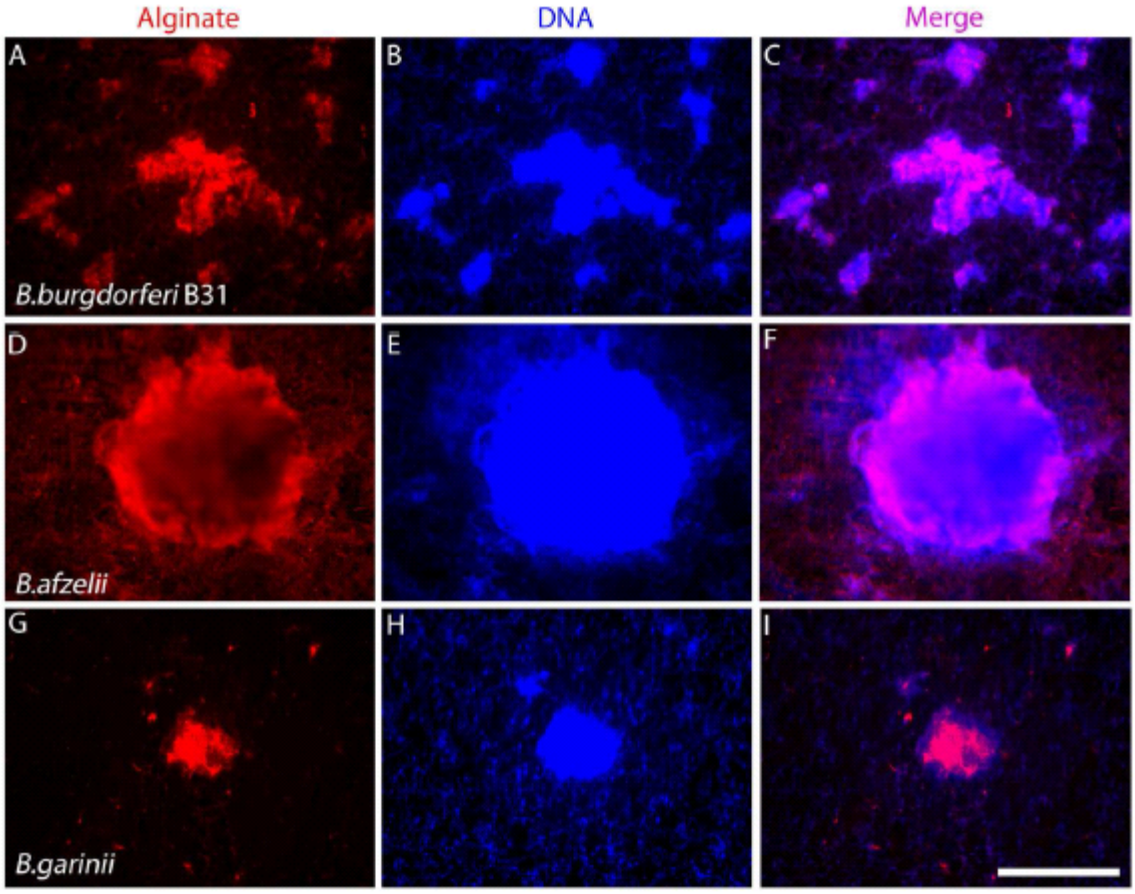

461

462 **Fig 5.** *Borrelia* aggregates contain an alginate rich matrix. Representative fluorescent micrographs A-
463 C *Borrelia burgdorferi* B31, D-F *Borrelia afzelii* and G-I *Borrelia garinii* aggregates, with anti-alginate
464 antibody (red) and DAPI (blue) and the respective merged maximum intensity projections show the
465 presence of alginate rich EPS.

466

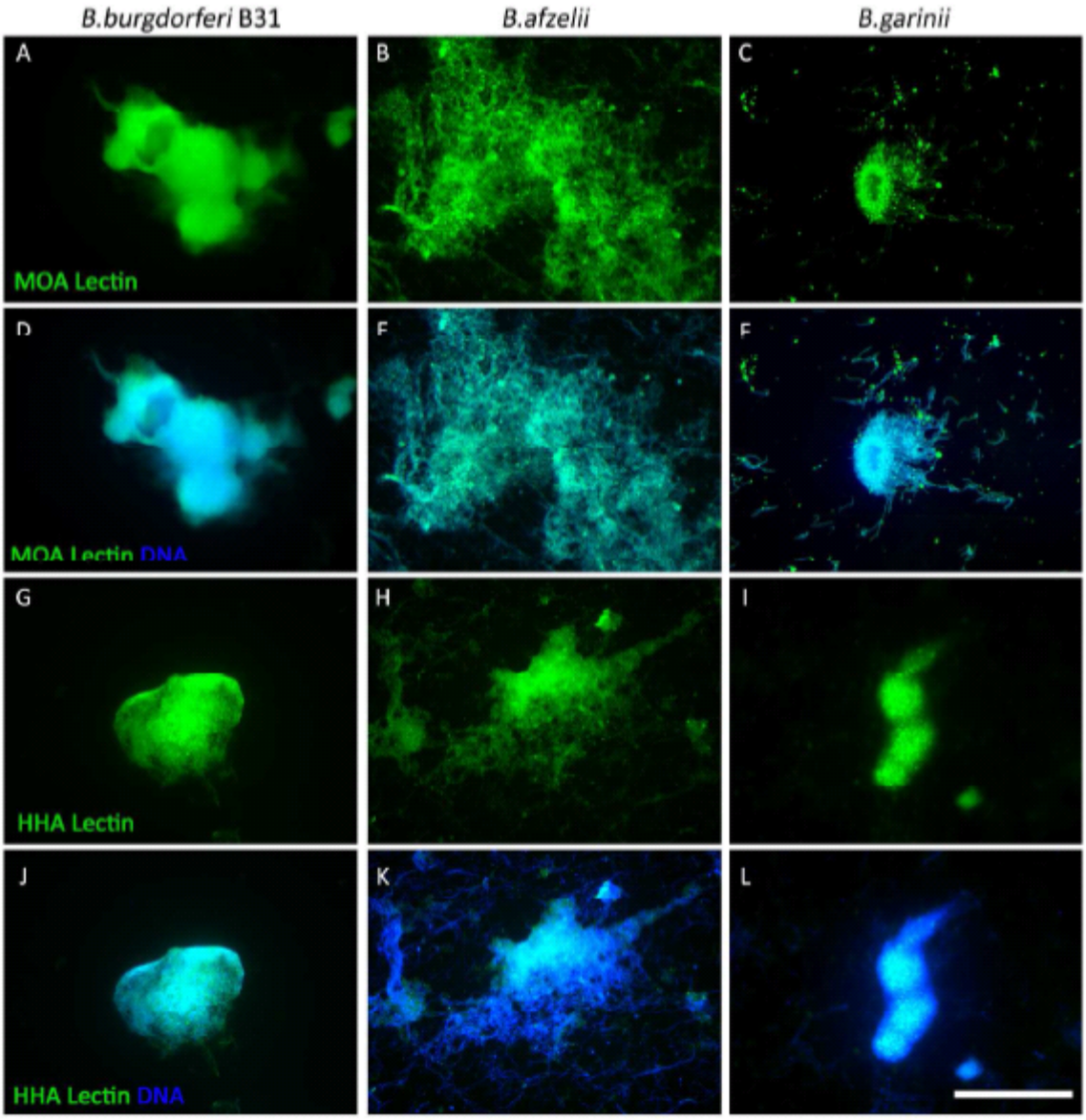

466

467 **Fig 6.** Borrelia aggregates contain a Psl-like polysaccharide. Representative fluorescent micrographs
468 of (A, D, G, J) *Borrelia burgdorferi* (B, E, H, K) *Borrelia afzelii* and (C, F, I, L) *Borrelia garinii* aggregates
469 stained with FITC conjugated HHA or MOA lectins (green) and DNA stained with DAPI (blue), show
470 the presence of a Psl-like polysaccharide. Scale bar - 100 µm.

471

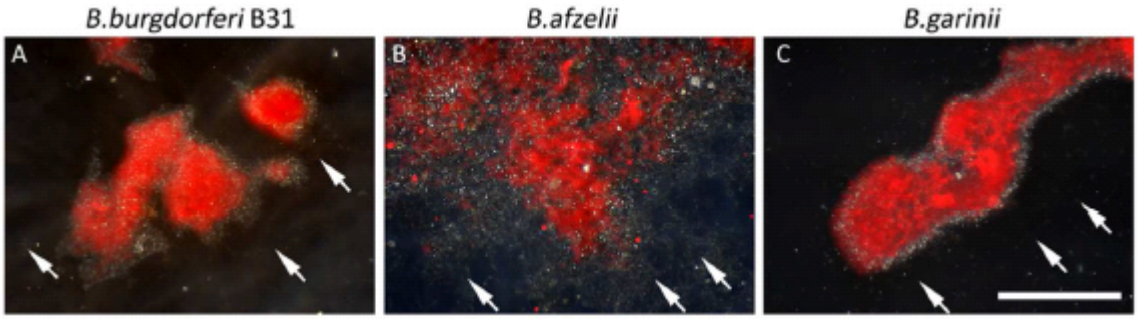

Fig 7. Presence of calcium in Borrelia aggregates. Representative dark field-fluorescence merged micrographs of Alizarin red S staining shows localization of calcium (red) in aggregates formed by (A) *Borrelia burgdorferi* (B) *Borrelia afzelii* and (C) *Borrelia garinii*. Scale bar - 100 µm. Arrows show that individual spirochetes surrounding the biofilm do not stain for alizarin red.

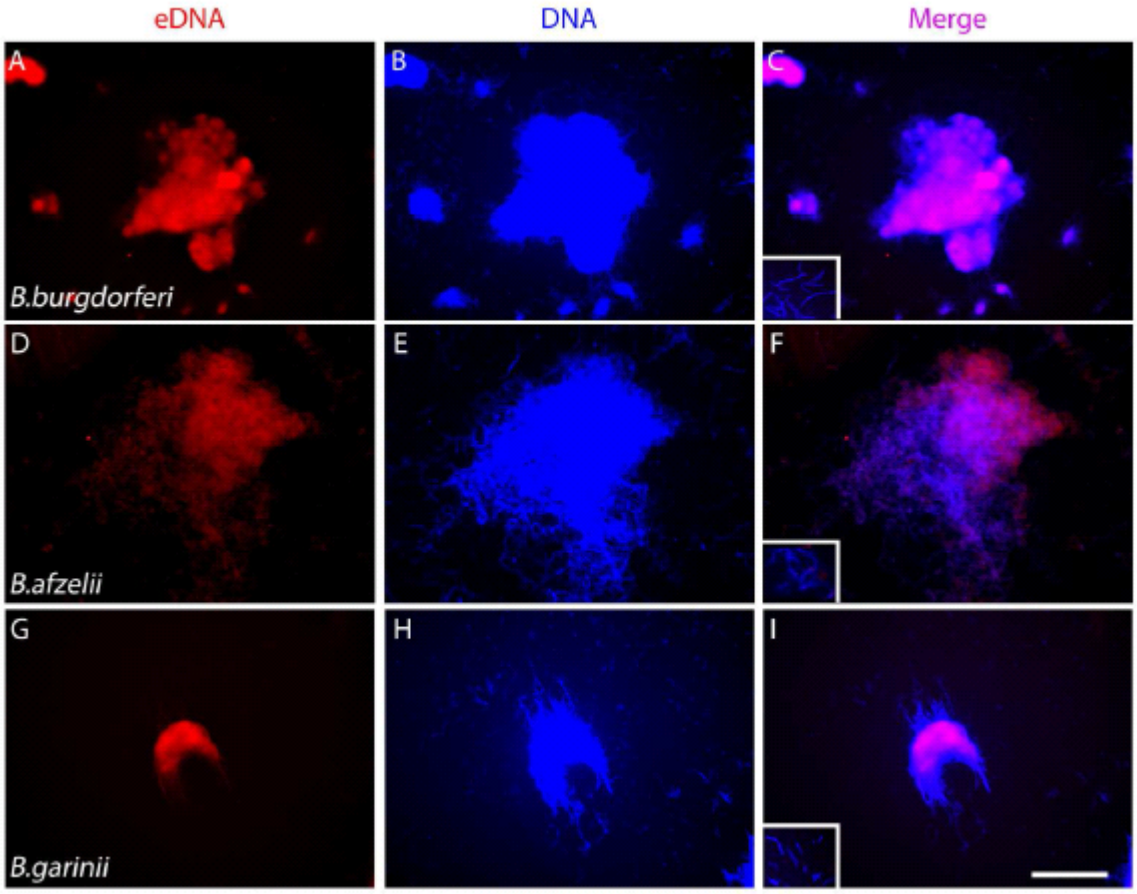

476

477 **Fig 8.** Presence of extracellular DNA in Borrelia aggregates but not in *Borrelia* spirochetes. Panels A-
478 C show representative fluorescent micrographs of DDAO stained *Borrelia burgdorferi* B31, *Borrelia*
479 *afzelii* and *Borrelia garinii* aggregates and spirochetes, respectively. DDAO eDNA staining – red, DAPI
480 DNA staining – blue. Scale bar - 100 µm. Inserts show individual spirochetes that do not stain for
481 eDNA.

482